Check for updates

Geophysical Research Letters

RESEARCH LETTER
10.1029/2026GL124518

Observational Evidence for Accelerated Warming and Salinification Propagating Into the Deep Mediterranean

Elena Terzić[1] and **Ivica Vilibić**[1,2]

[1]Division for Marine and Environmental Research, Ruđer Bošković Institute, Zagreb, Croatia, [2]Institute for Adriatic Crops and Karst Reclamation, Split, Croatia

Key Points:

- Mediterranean warming and salinification are accelerating, by up to 0.3°C per decade^2 in the upper 1,000–2,000 m
- Acceleration is vertically coherent, reaching the deep basin, so linear trends alone understate Mediterranean change
- Acceleration peaks in the Adriatic–Ionian dense-water sector, identifying it as an early indicator of basin-scale change

Supporting Information:

Supporting Information may be found in the online version of this article.

Correspondence to:

E. Terzić,
eterzic@irb.hr

Citation:

Terzić, E., & Vilibić, I. (2026). Observational evidence for accelerated warming and salinification propagating into the deep Mediterranean. *Geophysical Research Letters*, *53*, e2026GL124518. https://doi.org/10.1029/2026GL124518

Received 27 MAY 2026
Accepted 7 AUG 2026

Author Contributions:

Conceptualization: Elena Terzić, Ivica Vilibić
Data curation: Elena Terzić
Formal analysis: Elena Terzić
Funding acquisition: Ivica Vilibić
Investigation: Elena Terzić, Ivica Vilibić
Methodology: Elena Terzić, Ivica Vilibić
Project administration: Ivica Vilibić
Resources: Ivica Vilibić
Supervision: Ivica Vilibić
Validation: Elena Terzić
Visualization: Elena Terzić
Writing – original draft: Elena Terzić, Ivica Vilibić

© 2026 The Author(s). Geophysical Research Letters published by Wiley Periodicals LLC on behalf of American Geophysical Union.
This is an open access article under the terms of the Creative Commons Attribution License, which permits use, distribution and reproduction in any medium, provided the original work is properly cited.

Abstract Acceleration, rather than a gradual linear response, is emerging as a defining feature of ocean change in the Anthropocene. Surface-forced warming propagates into the deep ocean over decades to centuries, but semi-enclosed basins such as the Mediterranean Sea may respond more rapidly. Here, we analyse an in situ Mediterranean-wide multiplatform data set spanning 1950–2025 and show that warming and salinification of the upper 1,000–2,000 m are not only continuing but accelerating, at increasing rates over the record. Acceleration rates reach up to 0.3°C decade^{-2} for temperature and 0.1 decade^{-2} for salinity. Coastal shallow basins exhibit additional acceleration in processes that precondition changes in deep basins, including warming of dense waters that cascade to the deep Mediterranean. These results indicate rapid, ongoing changes in Mediterranean water-mass properties and position the basin as a natural laboratory for detecting and constraining accelerating ocean change.

Plain Language Summary The ocean is changing as it absorbs heat and responds to shifts in evaporation, rainfall, and circulation caused by climate change. These changes are often described as gradual trends, but in reality the rate of change itself may also be increasing. This is difficult to detect from observations, especially below the surface, because long records are sparse and modern measurements come from different observing systems. The Mediterranean Sea is a useful place to study this problem because it is relatively small, strongly affected by the atmosphere, and has a long history of oceanographic observations. We combine historical profiles, Argo float measurements, and regional observations from 1950 to 2025 to examine changes in temperature, salinity, and density throughout the Mediterranean water column. We find that warming and salinification are not only widespread, but accelerating, with signals extending from the surface into intermediate and deep waters. These changes are strongest near the surface and in regions connected to dense-water formation, where surface conditions can influence the deep sea. Our results suggest that the Mediterranean may provide an early indication of how quickly the properties of ocean basins can change under continued climate forcing.

1. Introduction

The global ocean is undergoing rapid changes in temperature, salinity, and density structure in response to anthropogenic climate forcing (IPCC, 2022; Masson-Delmotte et al., 2023). These changes alter ocean circulation (Wang et al., 2024), stratification (Cheng et al., 2025), and biogeochemical cycles (Keeling et al., 2010), with far-reaching consequences for climate (Pan et al., 2026) and marine ecosystems (Tan et al., 2026). Ocean change is, however, still commonly summarized in terms of linear trends, even though global assessments increasingly document rates of warming and sea-level rise that intensify over time (Masson-Delmotte et al., 2023; von Schuckmann et al., 2024).

Evidence is thus growing that rates of warming and salinification evolve over time (Cheng et al., 2017, 2022; Storto & Yang, 2024). The extent to which such changes are accelerating, and how this acceleration is distributed across depths and regions, remains poorly constrained. This limitation arises both from incomplete observational coverage, particularly the transition from sparse historical sampling to modern autonomous observing systems (Roemmich et al., 2019), and from the challenges of integrating heterogeneous data sets into consistent long-term records (Boyer et al., 2013; Iona et al., 2018).

The Mediterranean Sea provides a natural laboratory to investigate these processes. As a semi-enclosed basin with complex circulation and strong air–sea coupling, it exhibits high sensitivity to atmospheric forcing (A. R. Robinson & Golnaraghi, 1994; Schroeder et al., 2017), particularly in its eastern regions (Malanotte-Rizzoli

Writing – review & editing: Elena Terzić, Ivica Vilibić

et al., 2003). At the same time, it is among the best-observed ocean basins, with hydrographic records spanning over more than a century (Iona et al., 2018; Manca et al., 2004; Rixen et al., 2005), now complemented by modern observing systems such as Argo floats (Kassis & Korres, 2020; Kubin et al., 2023; Roemmich et al., 2019). The Mediterranean is also recognized as a climate change hot spot (Giorgi, 2006; Tuel & Eltahir, 2020), where warming and salinification rates exceed the global ocean average (Skliris et al., 2024; Somot et al., 2006; Soto-Navarro et al., 2020). These changes have the potential to impact dense water formation and basin-scale circulation (Parras-Berrocal et al., 2023; Somot et al., 2006; Verri et al., 2024).

Yet, whether hydrographic changes in this basin are indeed accelerating, and how such acceleration manifests across the full water column, has not been systematically quantified. Here we compile a multi-platform observational data set spanning 1950–2025 from historical hydrographic profiles, Argo observations, and regional in situ measurements. Using this data set, we quantify differences between the 20th and 21st centuries as a descriptive climatological contrast, assess long-term trends, and explicitly quantify acceleration in temperature, salinity, and potential density anomaly (PDA) by fitting a second-order polynomial over the full 1950–2025 record. Throughout, "acceleration" is used in a descriptive statistical sense, denoting a departure from a constant linear rate of change as quantified by the curvature of the quadratic fit. We provide evidence that these changes are not only widespread but also accelerating, with signals extending from the surface to deep waters, indicating a basin-scale transformation of water-mass properties in which accelerating responses to climate forcing can be detected early.

2. Materials and Methods

We compiled a multi-platform hydrographic data set spanning 1950–2025, combining SeaDataNet historical profiles (CTD, bottle, and MBT/XBT casts), Argo observations, and regional in situ measurements from the Adriatic Sea. Only observations carrying source quality-control flags "good" or "probably good" were retained, complemented by physically based range screening, and all data sets were harmonized to common temperature, salinity, depth, and time conventions. A complete description of the data sources, quality-control criteria, harmonization steps, and processing workflow is provided in Texts S1.1–S1.3 in Supporting Information S1.

For basin-scale analyses, individual Manca regions used in previous Mediterranean climatological analyses (Manca et al., 2004) were aggregated into 12 composed basins (Figure S1 in Supporting Information S1; the composition of each aggregated basin in terms of the original Manca regions is listed in Table S1 and Text S1.2 in Supporting Information S1). This framework was used for diagnostics requiring enhanced sampling robustness, including Hovmöller analyses, seasonal climatologies, temperature–salinity distributions, and vertical trend and acceleration estimates. Spatial maps (Figures 2a–2c and 3) are instead shown at the native, non-aggregated Manca-basin resolution to preserve regional structure; all time-series, climatological, and vertical diagnostics use the aggregated basins.

For selected depth-resolved diagnostics, three representative basins with sufficient deep coverage were analysed: the Northwestern Mediterranean, Ionian Sea, and Levantine Basin (defined in Table S1 in Supporting Information S1 and mapped in Figure S1 in Supporting Information S1). These basins capture the main west–central–east gradient of Mediterranean hydrographic regimes and distinct circulation and water-mass formation characteristics. Corresponding diagnostics for the remaining basins are provided in Supporting Information S1 (Figures S2–S16).

Coastal and estuarine influences were minimized using a 2 km distance-based mainland coastline mask and by excluding major river-influenced regions (Ludwig et al., 2009). To combine heterogeneous observations, we adopted depth-bin averaging centered on standard oceanographic levels (5–5,000 m; Table S2 and Text S1.3 in Supporting Information S1), rather than profile-wise interpolation. This uses only observed values within predefined depth intervals, reducing sensitivity to irregular vertical sampling. Temperature and salinity were accumulated independently within each bin, allowing temperature-only profiles (e.g., MBT/XBT casts) to contribute.

Seasonal climatologies were constructed using a two-pass approach following established Mediterranean frameworks (Manca et al., 2004), with outlier filtering based on variability within each basin, season, and depth level (Text S1.4 in Supporting Information S1). Data coverage was quantified using an "eligible cast" framework,

19448007, 2026, 18, Downloaded from https://agupubs.onlinelibrary.wiley.com/doi/10.1029/2026GL124518 by Cochrane Croatia, Wiley Online Library on [15/10/2026]. See the Terms and Conditions (https://onlinelibrary.wiley.com/terms-and-conditions) on Wiley Online Library for rules of use; OA articles are governed by the applicable Creative Commons License

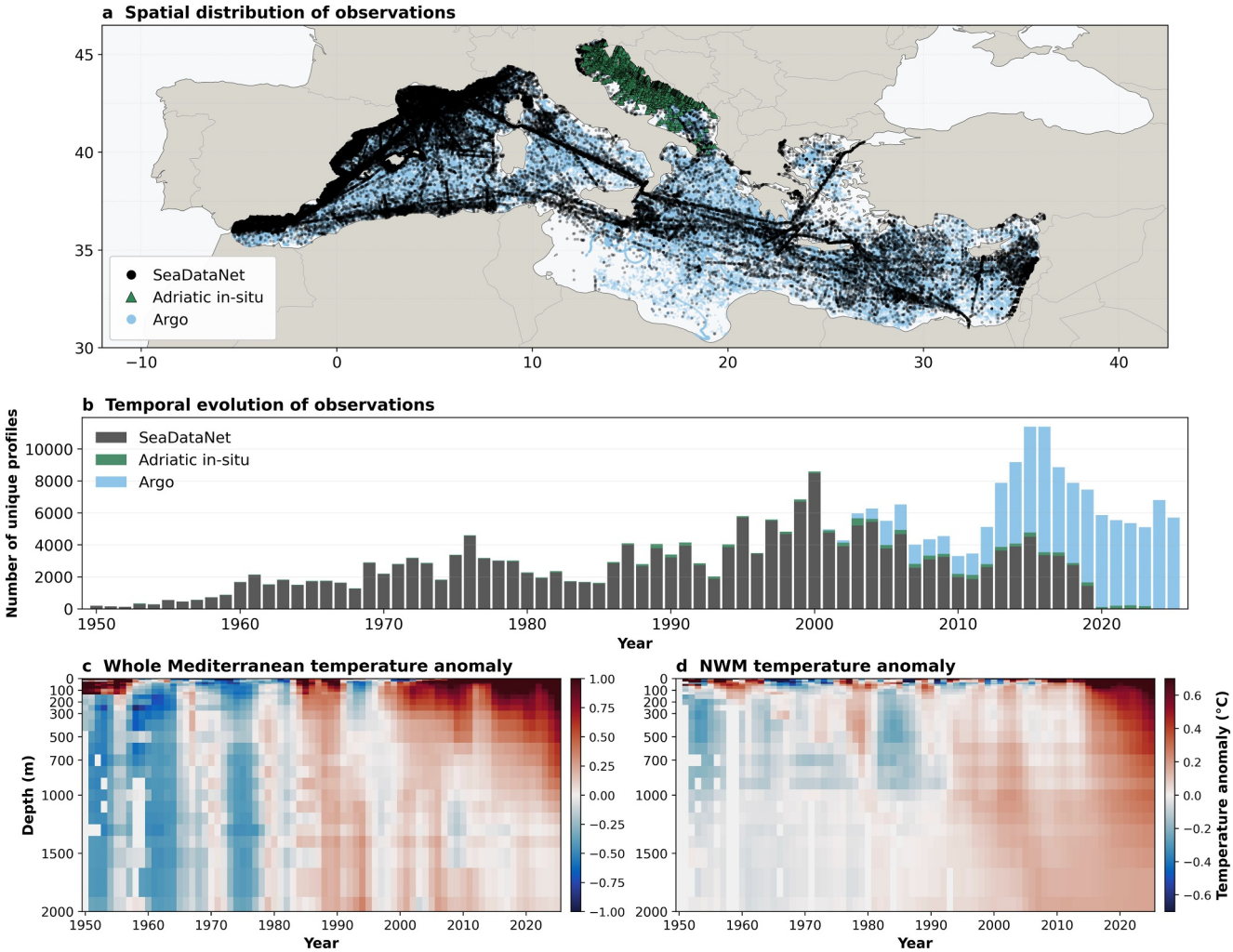

Figure 1. Observational data set and basin-wide changes. (a) Spatial distribution of observations (SeaDataNet, Argo, and regional Adriatic in situ data sets). (b) Unique profiles per year by data source. (c) Basin-integrated temperature anomaly versus depth and time for the entire Mediterranean (1950–2025) and (d) for the Northwestern Mediterranean (NWM); anomalies in (c–d) are relative to the 1950–1999 mean, smoothed with a 3-year running mean.

in which only profiles intersecting a given depth bin are included in the denominator, ensuring that sampling support reflects actual depth coverage.

Long-term changes were quantified from deseasoned monthly mean time series (per basin, depth bin, and variable; annual and semi-annual harmonics removed by ordinary least squares, OLS). Three complementary diagnostics, interpreted separately, were then computed (full detail in Texts S1.5 and S1.6 in Supporting Information S1). First, a descriptive climatological contrast between the 20th (1950–1999) and 21st century (2000–2025), used only to map where and at which depths the mean state has changed (Figures 1c, 1d, and 2), independent of the trend and acceleration estimation. Second, full-period (1950–2025) quadratic fits, $y(t) = at^2 + bt + c$, from which we report the acceleration (second derivative, 2a, per decade^2) and the linear rate of change (first derivative at the record midpoint, b, per decade; for a quadratic model this equals the record-mean rate and is independent of the time origin); these are the quantities shown in Figures 3 and 4. Third, period-wise linear trends (1950–1999 and 2000–2025), used only in the robustness comparison of fitting approaches (Figure S18 in Supporting Information S1). Statistical significance was assessed from the OLS standard errors (two-sided tests). PDA was computed using TEOS-10 formulations (IOC, SCOR and IAPSO, 2010).

The robustness of these estimates to the analysis window, the fitting approach, and the historical-to-Argo sampling transition was assessed through three sensitivity tests, detailed in Text S1.7 in Supporting Information S1

19448007, 2026, 18, Downloaded from https://agupubs.onlinelibrary.wiley.com/doi/10.1029/2026GL124518 by Cochrane Croatia, Wiley Online Library on [15/10/2026]. See the Terms and Conditions (https://onlinelibrary.wiley.com/terms-and-conditions) on Wiley Online Library for rules of use; OA articles are governed by the applicable Creative Commons License

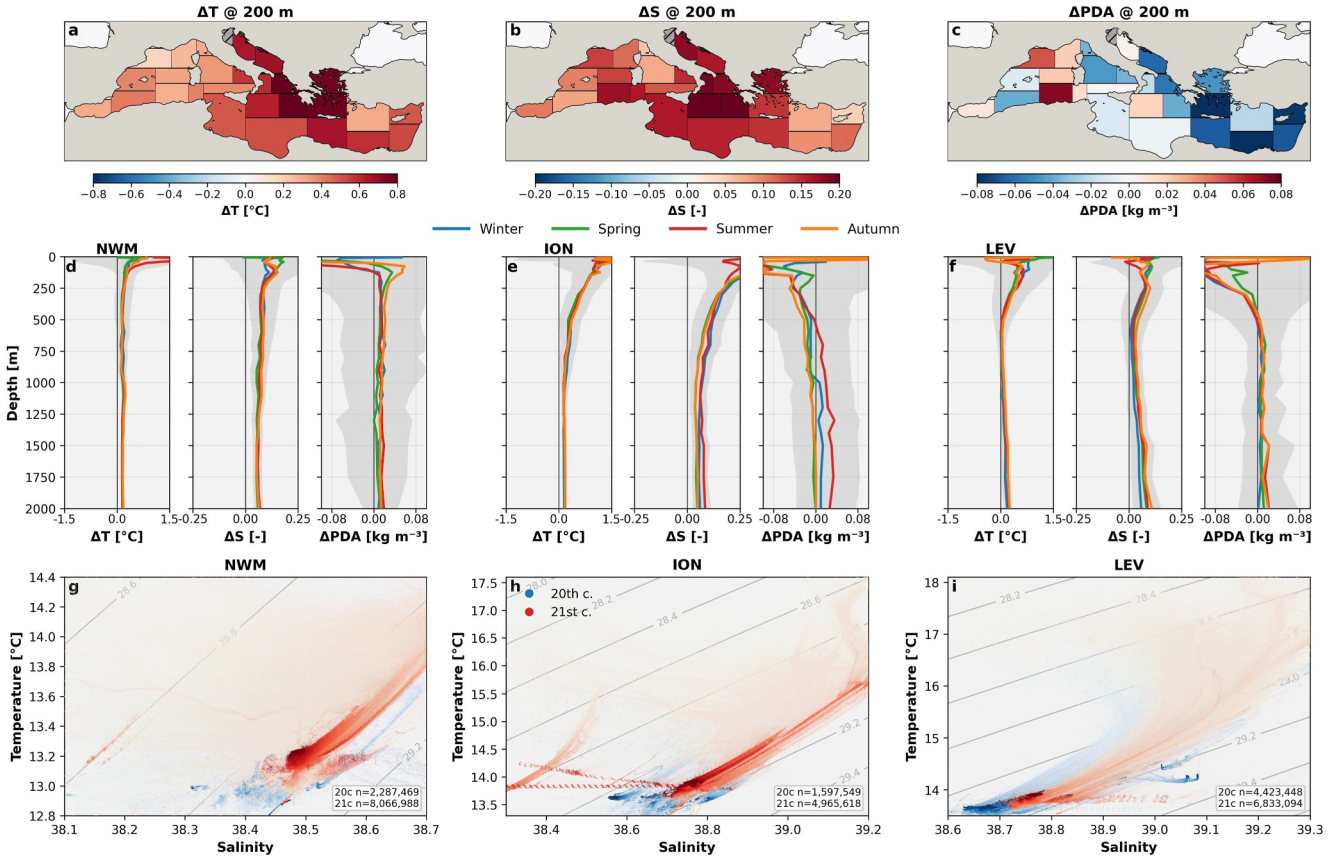

Figure 2. Basin-scale and vertical thermohaline differences between the 20th (1950–1999) and 21st century (2000–2025). (a–c) Differences at 200 m in temperature, salinity, and potential density anomaly (PDA). (d–f) Vertical profiles for the Northwestern Mediterranean, Ionian Sea, and Levantine Basin; colors denote seasonal differences. Gray shading is the combined seasonal ±1σ climatological spread, $\sigma = (\sigma_{21}^{2} + \sigma_{20}^{2})^{(1/2)}$ (per-season spreads in Figures S2–S13 in Supporting Information S1); near-surface values beyond the axis range are clipped. (g–i) Temperature–salinity distributions below the seasonal thermocline ($z > 100$ m) for the two periods, showing the displacement of water-mass properties; the number of casts is also shown.

(Figures S17–S19 and Figure 1b), which confirm that the sign and vertical structure of the reported signals are preserved.

The authors used ChatGPT (OpenAI) and Claude (Anthropic) for language editing, grammar correction, and improving the clarity of text drafted by the authors.

3. Results

3.1. Multi-Decadal Observations and Emerging Basin-Scale Signal

The compiled data set provides basin-wide, multi-decadal coverage across the Mediterranean (Figures 1a and 1b), combining irregular historical ship-based observations with dense Argo-era profiling. Sampling increases markedly after the early 2000 s, improving coverage of intermediate and deep layers, whereas earlier decades remain spatially heterogeneous. Despite these differences, including the transition to Argo-dominated observations, a coherent large-scale hydrographic signal emerges. Sampling support and platform composition are explicitly quantified per depth bin and period (Figure 1b and Figure S19 in Supporting Information S1), and the broad spatial and vertical patterns reported below remained robust across the sampling and fitting-window sensitivity tests conducted here (Figures S17 and S18 in Supporting Information S1). Basin-averaged temperature anomalies (Figure 1c) show persistent warming originating at the surface and propagating downward, evident basin-wide and illustrated here for the Northwestern Mediterranean (Figure 1d), a subbasin selected because deep convection is known to enable rapid vertical transfer of heat and salt (Somot et al., 2018; Testor et al., 2018);

19448007, 2026, 18, Downloaded from https://agupubs.onlinelibrary.wiley.com/doi/10.1029/2026GL124518 by Cochrane Croatia, Wiley Online Library on [15/10/2026]. See the Terms and Conditions (https://onlinelibrary.wiley.com/terms-and-conditions) on Wiley Online Library for rules of use; OA articles are governed by the applicable Creative Commons License

19448007, 2026, 18, Downloaded from https://agupubs.onlinelibrary.wiley.com/doi/10.1029/2026GL124518 by Cochrane Croatia, Wiley Online Library on [15/10/2026]. See the Terms and Conditions (https://onlinelibrary.wiley.com/terms-and-conditions) on Wiley Online Library for rules of use; OA articles are governed by the applicable Creative Commons License

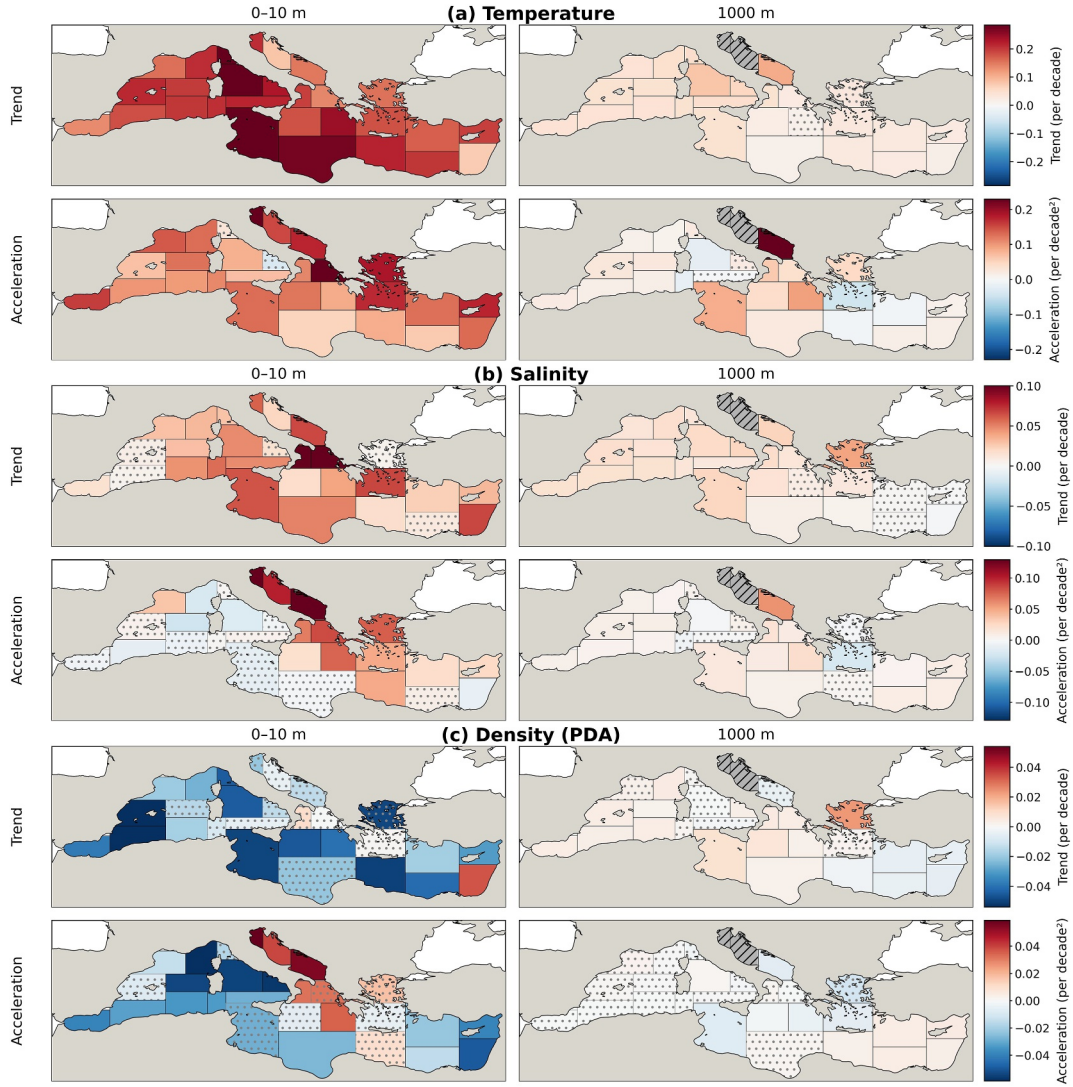

Figure 3. Trends and acceleration rates of the Mediterranean thermohaline properties. Full-period (1950–2025) linear rates of change (top row) and acceleration (bottom row) from the quadratic fits defined in Methods, for (a) temperature, (b) salinity, and (c) PDA, at the surface (0–10 m) and 1,000 m. Stippling marks non-significant trends ($p \geq 0.05$); hatching indicates ocean shallower than 1,000 m.

corresponding diagnostics for the other composed basins are provided in Figures S2–S13 in Supporting Information S1.

Temperature anomalies averaged within fixed depth layers (Figure 1c) peak in recent years, reaching ~2.04°C (0–100 m), ~1.13°C (100–300 m), and ~0.62°C (300–1,000 m), while remaining detectable at depth (~0.21°C at 1,000–2,000 m). The onset of persistent positive anomalies occurs progressively later with depth, indicating downward propagation. The Northwestern Mediterranean shows a similar but more surface-intensified structure (~2.19°C at the surface, ~0.24°C at 1,000–2,000 m), again emerging later at depth.

3.2. Basin-Scale Differences Between the 20th and 21st Centuries

Century-scale differences (21st vs. 20th) reveal widespread warming and salinification across the Mediterranean, strongest in the upper and intermediate layers but extending into the deep basin (Figure 2). The two periods are predefined climatological intervals: the longer historical interval (1950–1999) preserves sufficient observational support in the sparsely sampled pre-Argo era, particularly at depth, while the modern interval (2000–2025) is Argo-dominated (Figure 1b and Figure S19 in Supporting Information S1). This contrast is descriptive and

10.1029/2026GL124518

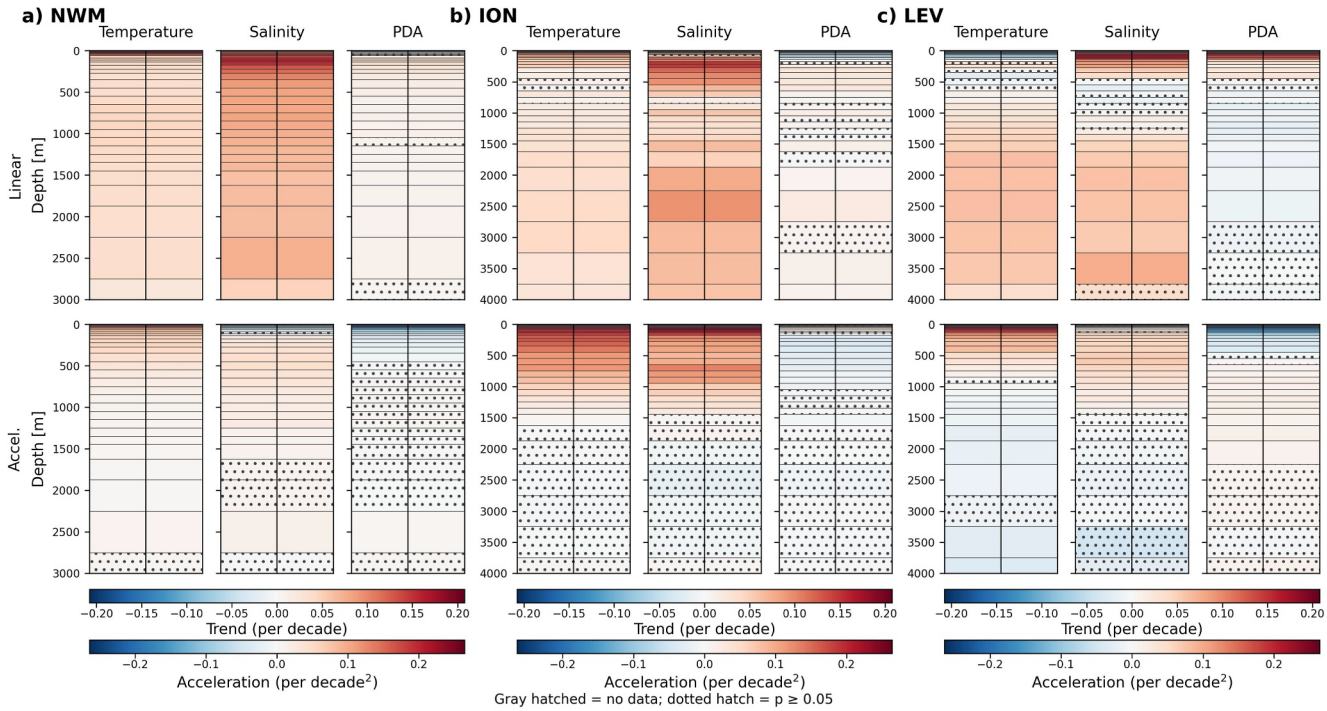

Figure 4. Vertical structure of thermohaline trends and acceleration rates across representative Mediterranean basins (1950–2025). Vertical profiles of temperature (°C), salinity, and PDA (kg m^{-3}) for the Northwestern Mediterranean (NWM), Ionian Sea (ION), and Levantine Basin (LEV), extending to the deepest sampled levels (~3,000 m in the NWM, ~4,000 m in the ION and LEV). Upper row: midpoint linear trend (per decade); lower row: acceleration (per $decade^2$), from the full-period quadratic fits defined in Methods. Warm and cool tones indicate positive and negative values; gray shading marks bins with insufficient coverage and dotted hatching non-significant trends ($p \geq 0.05$).

independent of the full-period trend and acceleration analyses (Section 3.3). At the surface (0–10 m), temperature differences reach ~1.42°C in the Northwestern Mediterranean (Figure 2a). At 200 m, corresponding to the core of Levantine Intermediate Water (LIW) (A. Robinson et al., 1992; Emelianov et al., 2006), maximum warming occurs in the Ionian Sea (~0.92°C). The 200 m level is used as the mapping reference because it lies below the seasonal thermocline, samples the LIW horizon, and retains high observational coverage across all basins; the corresponding vertical structure is shown in Figures 2d–2f.

Salinity shows a coherent but more eastern-intensified pattern (Figure 2b). Surface anomalies reach ~1.10 in the northern Aegean, while intermediate maxima occur in the Ionian Sea (~0.25 at 200 m; ~0.18 at 1,000 m). In the Levantine Basin, where LIW forms (Malanotte-Rizzoli et al., 2003), positive anomalies persist to depth (~0.11 at 2,000 m). In contrast, PDA changes are mostly negative and heterogeneous (Figure 2c), with weak deep signals, indicating compensation between temperature and salinity effects.

Seasonal profiles show the largest vertical offsets in the upper ~5–40 m (Figures 2d–2f). Temperature anomalies peak in summer in the Northwestern Mediterranean (~2.01°C at 20 m) and in autumn in the Ionian Sea (up to ~3.19°C at 5 m). Salinity anomalies are strongest in the Ionian Sea across seasons (to ~0.58 at 40 m in winter), extending from the surface to intermediate depths. PDA remains predominantly negative in the upper layer, especially in summer in the Northwestern Mediterranean (down to ~–0.52 at 20 m), indicating warming-driven lightening.

The temperature–salinity distributions (Figures 2g–2i) summarize these changes as displacements of water-mass properties between the two periods: below the seasonal thermocline, the 21st-century distributions are systematically shifted toward warmer and saltier classes. In temperature–salinity space, the largest 21st–20th century displacement occurs in the Ionian Sea, with median shifts of $\Delta T \sim 1.27$°C and $\Delta S \sim 0.26$ in the 100–300 m layer, exceeding those in other basins. Together, these results indicate basin-wide warming and salinification alongside a marked transformation of intermediate and deep water-mass properties, particularly in the

19448007, 2026, 18, Downloaded from https://agupubs.onlinelibrary.wiley.com/doi/10.1029/2026GL124518 by Cochrane Croatia, Wiley Online Library on [15/10/2026]. See the Terms and Conditions (https://onlinelibrary.wiley.com/terms-and-conditions) on Wiley Online Library for rules of use; OA articles are governed by the applicable Creative Commons License

19448007, 2026, 18, Downloaded from https://agupubs.onlinelibrary.wiley.com/doi/10.1029/2026GL124518 by Cochrane Croatia, Wiley Online Library on [15/10/2026]. See the Terms and Conditions (https://onlinelibrary.wiley.com/terms-and-conditions) on Wiley Online Library for rules of use; OA articles are governed by the applicable Creative Commons License

Adriatic–Ionian–Levantine sector (Civitarese et al., 2023; Eusebi Borzelli & Carniel, 2023), where dense-water formation and quasi-decadal circulation variability are known to redistribute heat and salt (Gačić et al., 2010).

3.3. Accelerating the Temperature and Salinity Increase

Thermohaline changes in the Mediterranean are not steady but accelerating across basins (Figure 3). Full-period (1950–2025) rates of change, estimated as the midpoint derivative of the quadratic fit (equivalent to the record-mean rate; Section 2), show coherent surface (0–10 m) warming across nearly all sub-basins, locally exceeding ∼0.30°C per decade and peaking in the Northwestern Mediterranean. This signal persists at 1,000 m (∼0.11°C per decade), with a maximum in the southern Adriatic Sea. The acceleration term reveals pronounced departures from a constant rate of change, with largest surface values occurring in the Adriatic and northern Ionian (>0.2°C per decade^2), while at depth acceleration remains basin-wide, again strongest in the southern Adriatic (∼0.23°C per decade^2). This is consistent with rapid warming and salinification of dense waters cascading from the shallow northern Adriatic (Martellucci et al., 2025; Terzić, Cardin, et al., 2025). In contrast, weak negative acceleration in the southern Aegean is consistent with the legacy of the warmer- and saltier-than-average waters generated during the Eastern Mediterranean Transient (Incarbona et al., 2016; Roether et al., 2007).

Salinity exhibits similar but regionally differentiated behavior. Surface salinification is widespread, strongest in the central and eastern basins, particularly the Adriatic (∼0.11 per decade). At 1,000 m, trends are smaller (∼0.04 per decade) but predominantly positive, while acceleration peaks again in the southern Adriatic (∼0.06 per decade^2), reinforcing its role as a hotspot of accelerating change. The combined thermohaline signal is reflected in PDA: surface trends are weak or negative (to ∼–0.06 kg m^{-3} per decade), indicating temperature dominance, whereas at depth they become weakly positive (∼0.02 kg m^{-3} per decade), consistent with increasing salinity influence. Positive PDA acceleration in the Adriatic–Ionian region (to ∼0.13 kg m^{-3} per decade^2 at the surface) indicates that salinity-driven densification increasingly offsets warming, though this weakens at 1,000 m. For temperature and salinity the linear and quadratic descriptions agree at large scale; for density, however, the acceleration term reveals an evolving warming–salinification compensation not apparent from the rates of change alone.

The vertical structure of trends and acceleration across the three representative basins is resolved in Figure 4, which extends to ∼3,000 m in the Northwestern Mediterranean and ∼4,000 m in the Ionian and Levantine basins, covering the deep and, where sampled, abyssal layers (remaining basins: Figures S14–S16 in Supporting Information S1). In the Ionian and Levantine basins, warming acceleration reaches the deep interior, so the acceleration signal penetrates through much of the water column.

Temperature trends are positive throughout most of the water column (except near-surface in the Levantine, below) and exhibit a clear decay with depth while remaining significant to at least ∼3,000 m. Surface warming reaches ∼0.23°C per decade in the Ionian basin and ∼0.21°C per decade in the Northwestern Mediterranean at ∼10 m, while intermediate values remain substantial (e.g. ∼0.06°C per decade at 75–100 m). Positive trends persist into the deep ocean (to ∼0.03–0.04°C per decade).

Salinity trends are weaker but vertically coherent. Although surface salinity trends appear spatially patchier than temperature in the sub-basin maps (Figure 3b), they are more vertically persistent (Figure 4), remaining positive and significant over much of the water column. In the Ionian basin, they peak near the surface (∼0.05 per decade) and remain positive at depth. The Levantine basin shows surface-intensified salinification (∼0.06 per decade), while the Northwestern Mediterranean exhibits weaker intermediate-depth maxima (∼0.03 per decade).

In the Ionian and Northwestern Mediterranean basins, PDA trends are negative in the upper ∼50 m (to ∼–0.05 kg m^{-3} per decade) but become positive below ∼200 m. In contrast, the Levantine basin shows positive PDA trends already in the upper layer (∼0.10 kg m^{-3} per decade) before weakening at depth. Here, record-mean warming is weak or slightly negative in the upper ∼100 m. The warming acceleration is nonetheless the strongest of the three basins (∼0.24–0.29°C per decade^2), indicating a shift from mid-record cooling to rapid recent warming. Combined with surface-intensified salinification, this allows densification to reach ∼400–500 m. In the Northwestern Mediterranean and Ionian, near-surface warming and salinification instead compensate, so salinity-driven densification emerges only at depth, most clearly in the Ionian.

Temperature acceleration is strongest in the upper ocean (∼0.26–0.29°C per decade^2) but remains significant through intermediate depths and into the deep ocean. Salinity acceleration is smaller and primarily confined to

surface and intermediate layers, while PDA acceleration is generally negative in these layers. The negative near-surface PDA acceleration indicates that warming increasingly outpaces salinification in the upper ocean, a tendency toward reduced surface density that could make preconditioning for dense-water formation less efficient, though assessing this requires dedicated process studies.

Together, these results show that Mediterranean thermohaline changes are widespread, accelerating, and vertically coherent. The fitted rates of change are significant across most sub-basins, the quadratic terms are themselves significant, and both retain consistent signs and vertical structure from the surface to depth. These properties are linked: a surface signal that is both strong and strengthening imposes a correspondingly large signal on the layers below, which in turn communicate it to the interior. Intermediate depths (~75–300 m) accordingly act as a transition zone linking surface forcing to the ocean interior, where both trends and acceleration remain strong. The persistence of coherent signals at depth indicates basin-scale changes in thermohaline properties across much of the water column, extending below 2,000 m where observational coverage permits (Figure 4 and Figures S14–S16 in Supporting Information S1).

4. Discussion and Conclusions

Our results demonstrate that thermohaline change in the Mediterranean Sea is not a steady, surface-confined process, but a vertically coherent and accelerating response extending from the surface into intermediate and deep layers. This finding adds a depth-resolved, basin-scale perspective to the growing evidence that rates of ocean change are increasing globally (Masson-Delmotte et al., 2023; von Schuckmann et al., 2024; Storto & Yang, 2024). The consistency of this signal across basins, despite major shifts in observational systems between the historical and Argo eras, indicates a basin-scale signal rather than an observational artifact (Figures S17–S19 in Supporting Information S1).

The vertical coherence of trends and acceleration rates suggests that the observed changes are not confined to the directly forced surface layer, and is consistent with a redistribution of heat, salt, and water-mass properties throughout the basin by ventilation, advection, mixing, and water-mass transformation. In particular, recent analyses of the Mediterranean overturning circulation emphasize the role of boundary currents and boundary–interior exchanges, alongside open-ocean deep convection, in ventilating intermediate and deep layers (Kubin et al., 2019; Pinardi et al., 2019; Waldman et al., 2018); such pathways provide a physically consistent route by which surface-intensified anomalies can reach the basin interior, although our analyses do not resolve the individual redistribution mechanisms. Changes in upper-ocean stratification may further modulate this coupling: the increasing occurrence of marine heatwaves (Darmaraki et al., 2019; Juza et al., 2022) and the deepening of surface high-salinity layers, the so-called surface saline lakes, (Terzić, Gardiol, & Vilibić, 2025) both act on the surface buoyancy field that preconditions ventilation and may thereby influence how efficiently anomalies are transferred to depth.

Regional contrasts highlight the role of basin-specific dynamics in shaping the observed response. The Adriatic–Ionian system emerges as a focal region of accelerating change. This behavior is consistent with the role of the southern Adriatic as a key site of dense water formation and rapid ventilation (A. Robinson et al., 1992). The pronounced variability observed in the Ionian Sea is also consistent with its known quasi-decadal circulation reversals (Gačić et al., 2010), which may enhance the redistribution of heat and salt. In contrast, the Levantine Basin exhibits a more surface-intensified response, reflecting differences in ventilation pathways and water-mass residence times (Margirier et al., 2020). Local deviations, including negative accelerations in parts of the Aegean Sea, may be linked to episodic large-scale events such as the Eastern Mediterranean Transient (EMT) (Incarbona et al., 2016; Roether et al., 2007), which fundamentally altered intermediate and deep water formation. The EMT itself reflected a shift in dense-water production between competing Adriatic and Aegean sources; the pronounced warming and salinification of southern-Adriatic dense waters and the near-surface Levantine densification documented here are consistent with ongoing changes in the properties these sources supply, though our analyses do not resolve the associated circulation adjustments.

The combined warming and salinification imply a sustained transformation of the basin's water-mass properties, with implications for stratification, mixing, and the stability of intermediate and deep waters. The increasing contribution of salinity to density at depth suggests modifications in densification processes, consistent with projections of future Mediterranean evolution under climate change scenarios (Richon et al., 2019; Tuel & Eltahir, 2020).

19448007, 2026, 18, Downloaded from https://agupubs.onlinelibrary.wiley.com/doi/10.1029/2026GL124518 by Cochrane Croatia, Wiley Online Library on [15/10/2026]. See the Terms and Conditions (https://onlinelibrary.wiley.com/terms-and-conditions) on Wiley Online Library for rules of use; OA articles are governed by the applicable Creative Commons License

19448007, 2026, 18, Downloaded from https://agupubs.onlinelibrary.wiley.com/doi/10.1029/2026GL124518 by Cochrane Croatia, Wiley Online Library on [15/10/2026]. See the Terms and Conditions (https://onlinelibrary.wiley.com/terms-and-conditions) on Wiley Online Library for rules of use; OA articles are governed by the applicable Creative Commons License

While long-term Mediterranean warming and salinification have been widely documented (Kubin et al., 2023), the vertically coherent acceleration identified here shows that the rate of change is itself changing (Li et al., 2023; Storto & Yang, 2024). Given its relatively rapid turnover and strong sensitivity to atmospheric forcing, the basin may be viewed as an early indicator of accelerating ocean response to sustained climate forcing (Schroeder & Chiggiato, 2023). Linear trend-based frameworks may therefore underestimate both the magnitude and rate of future change; accounting for time-varying rates is essential for projecting the ocean's response to ongoing climate forcing.

The processes responsible for the detected acceleration remain to be quantified: changes in air–sea heat and freshwater fluxes, exchanges through the Strait of Gibraltar, freshwater inputs, and internal redistribution by the thermohaline circulation are all plausible contributors. Disentangling their relative roles would require homogeneous long-term atmospheric and surface-flux products together with water-mass transformation diagnostics, and is a target for future process-oriented studies; the present analysis provides the observational constraint on which such attribution can build. The accelerating, non-stationary behavior documented here also motivates dedicated investigation of the underlying nonlinear dynamical processes, which would require analyses of the governing mechanisms and forcing–response relationships (Ghil et al., 2002) beyond the scope of this observational Letter.

A further limitation concerns spatial coverage: like most Mediterranean observational compilations, our data set samples the Tunisian–Algerian coastal region only sparsely (Figure 1a). The impact on the basin-scale physical diagnostics reported here is likely minor, as the signals we describe are spatially coherent across neighboring subbasins. The gap is more consequential for biogeochemical processes, nutrient dynamics, and fisheries in a region of considerable ecological and economic importance, and closing it remains a priority for future observation.

Inclusion in Global Research Statement

This study uses publicly available international observing-system data and regional in situ observations from the Mediterranean Sea. The research was led by scientists based in the region where the study was conducted, and the authorship reflects the contributions to study design, data analysis, interpretation, and manuscript preparation. No field permits, community permissions, or formal agreements with local communities were required for this study.

Acknowledgments
We thank the two anonymous reviewers for their careful and constructive comments, which substantially improved the manuscript. In accordance with AGU's data policy, all data and software needed to evaluate and reproduce the results of this study are openly available or archived in the repositories identified in the Availability Statement section; no restricted or proprietary data were used. We thank the developers of the ArgoPy library for facilitating access to and analysis of Argo float data. The Argo data were collected and made freely available by the International Argo Program and the national programs that contribute to it. We also acknowledge the developers of the MapPlotter and Basins libraries for providing useful tools for visualization and spatial analysis. The work has been supported by Croatian Science Foundation through projects GLOMETS (Grant IP-2022-10-3064), C3PO (Grant IP-2022-9139), by Interreg Italy-Croatia 2021–2027 project AdriaClimPlus (Grant ITHR0200333), EU NextGeneration project AdriaClimRisk (Grant PK.3.4.17.0001), and the incoming mobility scheme for postdoctoral researchers (MOBDOL-2023-12, ET). The authors reviewed and approved all text and take full responsibility for the scientific content of the manuscript.

Conflict of Interest

The authors declare no conflicts of interest relevant to this study.

Availability Statement

Argo float observations used in this study are publicly available through the Argo Global Data Assembly Centre (Argo GDAC; Argo, 2000) and were accessed and processed using the ArgoPy Python library (Maze & Balem, 2020). Historical temperature and salinity observations were obtained from the SeaDataNet aggregated Mediterranean Sea data set, version 2 (IFREMER/IDM/SISMER et al., 2020). The cleaned regional Adriatic in situ data sets used in this study are archived in Zenodo (Terzić & Vilibić, 2026a). That record includes four cleaned Adriatic hydrographic CSV files and a README file documenting provenance, file mapping, row counts, file sizes, variables, and processing summary. The analysis code required to reproduce the main workflow and manuscript figures is archived in Zenodo (Terzić & Vilibić, 2026b). It comprises the analysis and plotting scripts used for preprocessing, quality control, basin-based climatology and time-series construction, trend and acceleration estimation, robustness analyses, and manuscript-figure generation, and contains the complete compilation and harmonization workflow for the multiplatform data set used here.

References

Argo. (2000). Argo float data and metadata from Global Data Assembly Centre (Argo GDAC) [Dataset]. *SEANOE*. https://doi.org/10.17882/42182

Boyer, T. P., Antonov, J. I., Baranova, O. K., Coleman, C., Garcia, H. E., Grodsky, A., et al. (2013). *World ocean database 2013* (Vol. 72). Silver Spring, MD: NOAA National Oceanographic Data Center. https://doi.org/10.7289/V5NZ85MT

Cheng, L., Abraham, J., Trenberth, K. E., Fasullo, J., Boyer, T., Mann, M. E., et al. (2022). Another record: Ocean warming continues through 2021 despite La Niña Conditions. *Advances in Atmospheric Sciences*, *39*(3), 373–385. https://doi.org/10.1007/s00376-022-1461-3

Cheng, L., Li, G., Long, S.-M., Li, Y., von Schuckmann, K., Trenberth, K. E., et al. (2025). Ocean stratification in a warming climate. *Nature Reviews Earth & Environment*, *6*(10), 637–655. https://doi.org/10.1038/s43017-025-00715-5

Cheng, L., Trenberth, K. E., Fasullo, J., Boyer, T., Abraham, J., & Zhu, J. (2017). Improved estimates of ocean heat content from 1960 to 2015. *Science Advances*, *3*(3), e1601545. https://doi.org/10.1126/sciadv.1601545

Civitarese, G., Gačić, M., Batistić, M., Bensi, M., Cardin, V., Dulčić, J., et al. (2023). The BiOS mechanism: History, theory, implications. *Progress in Oceanography*, *216*, 103056. https://doi.org/10.1016/j.pocean.2023.103056

Darmaraki, S., Somot, S., Sevault, F., Nabat, P., Cabos Narvaez, W. D., Cavicchia, L., et al. (2019). Future evolution of marine heatwaves in the Mediterranean Sea. *Climate Dynamics*, *53*(3–4), 1371–1392. https://doi.org/10.1007/s00382-019-04661-z

Emelianov, M., Font, J., Turiel, A., Millot, C., Solé, J., Poulain, P.-M., et al. (2006). Transformation of Levantine Intermediate Water tracked by MEDARGO floats in the Western Mediterranean. *Ocean Science*, *2*, 281–290. https://doi.org/10.5194/os-2-281-2006

Eusebi Borzelli, G. L., & Carniel, S. (2023). A reconciling vision of the Adriatic-Ionian Bimodal Oscillating System. *Scientific Reports*, *13*(1), 2334. https://doi.org/10.1038/s41598-023-29162-2

Gačić, M., Eusebi Borzelli, G. L., Civitarese, G., Cardin, V., & Yari, S. (2010). Can internal processes sustain reversals of the ocean upper circulation? The Ionian Sea example. *Geophysical Research Letters*, *37*(9), 2010GL043216. https://doi.org/10.1029/2010GL043216

Ghil, M., Allen, M. R., Dettinger, M. D., Ide, K., Kondrashov, D., Mann, M. E., et al. (2002). Advanced spectral methods for climatic time series. *Reviews of Geophysics*, *40*(1), 3-1–3-41. https://doi.org/10.1029/2000RG000092

Giorgi, F. (2006). Climate change hot-spots. *Geophysical Research Letters*, *33*(8), 2006GL025734. https://doi.org/10.1029/2006GL025734

IFREMER/IDM/SISMER, Simoncelli, S., Schaap, D., & Schlitzer, R. (2020). Mediterranean Sea—Temperature and salinity Historical Data Collection SeaDataCloud V2 (SDC_MED_DATA_TS_V2) [Dataset]. *SeaDataNet*. https://doi.org/10.12770/2a2aa0c5-4054-4a62-a18b-3835b304fe64

Incarbona, A., Martrat, B., Mortyn, P. G., Sprovieri, M., Ziveri, P., Gogou, A., et al. (2016). Mediterranean circulation perturbations over the last five centuries: Relevance to past Eastern Mediterranean Transient-type events. *Scientific Reports*, *6*(1), 29623. https://doi.org/10.1038/srep29623

IOC, SCOR and IAPSO. (2010). *The international thermodynamic equation of seawater—2010: Calculation and use of thermodynamic properties* (Tech. Rep. No. 56). UNESCO. https://doi.org/10.25607/OBP-1662

Iona, A., Theodorou, A., Watelet, S., Troupin, C., Beckers, J.-M., & Simoncelli, S. (2018). Mediterranean Sea Hydrographic Atlas: Towards optimal data analysis by including time-dependent statistical parameters. *Earth System Science Data*, *10*(3), 1281–1299. https://doi.org/10.5194/essd-10-1281-2018

IPCC. (2022). *The ocean and cryosphere in a changing climate: Special report of the intergovernmental panel on climate change* (1st ed.). Cambridge University Press. https://doi.org/10.1017/9781009157964

Juza, M., Fernández-Mora, À., & Tintoré, J. (2022). Sub-regional marine heat waves in the Mediterranean Sea from observations: Long-term surface changes, sub-surface and coastal responses. *Frontiers in Marine Science*, *9*, 785771. https://doi.org/10.3389/fmars.2022.785771

Kassis, D., & Korres, G. (2020). Hydrography of the Eastern Mediterranean basin derived from Argo floats profile data. *Deep Sea Research Part II: Topical Studies in Oceanography*, *171*, 104712. https://doi.org/10.1016/j.dsr2.2019.104712

Keeling, R. F., Körtzinger, A., & Gruber, N. (2010). Ocean deoxygenation in a warming world. *Annual Review of Marine Science*, *2*(1), 199–229. https://doi.org/10.1146/annurev.marine.010908.163855

Kubin, E., Menna, M., Mauri, E., Notarstefano, G., Mieruch, S., & Poulain, P.-M. (2023). Heat content and temperature trends in the Mediterranean Sea as derived from Argo float data. *Frontiers in Marine Science*, *10*, 1271638. https://doi.org/10.3389/fmars.2023.1271638

Kubin, E., Poulain, P.-M., Mauri, E., Menna, M., & Notarstefano, G. (2019). Levantine Intermediate and Levantine Deep Water formation: An Argo float study from 2001 to 2017. *Water*, *11*(9), 1781. https://doi.org/10.3390/w11091781

Li, Z., England, M. H., & Groeskamp, S. (2023). Recent acceleration in global ocean heat accumulation by mode and intermediate waters. *Nature Communications*, *14*(1), 6888. https://doi.org/10.1038/s41467-023-42468-z

Ludwig, W., Dumont, E., Meybeck, M., & Heussner, S. (2009). River discharges of water and nutrients to the Mediterranean and Black Sea: Major drivers for ecosystem changes during past and future decades? *Progress in Oceanography*, *80*(3–4), 199–217. https://doi.org/10.1016/j.pocean.2009.02.001

Malanotte-Rizzoli, P., Manca, B. B., Marullo, S., Ribera d' Alcala', M., Roether, W., Theocharis, A., et al. (2003). The Levantine intermediate water experiment (LIWEX) group: Levantine basin—A laboratory for multiple water mass formation processes. *Journal of Geophysical Research*, *108*(C9), 8101. https://doi.org/10.1029/2002JC001643

Manca, B., Burca, M., Giorgetti, A., Coatanoan, C., Garcia, M.-J., & Iona, A. (2004). Physical and biochemical averaged vertical profiles in the Mediterranean regions: An important tool to trace the climatology of water masses and to validate incoming data from operational oceanography. *Journal of Marine Systems*, *48*(1–4), 83–116. https://doi.org/10.1016/j.jmarsys.2003.11.025

Margirier, F., Testor, P., Heslop, E., Mallil, K., Bosse, A., Houpert, L., et al. (2020). Abrupt warming and salinification of intermediate waters interplays with decline of deep convection in the Northwestern Mediterranean Sea. *Scientific Reports*, *10*(1), 20923. https://doi.org/10.1038/s41598-020-77859-5

Martellucci, R., Paladini de Mendoza, F., Menna, M., Pirro, A., Reale, M., Gačić, M., et al. (2025). A multiobservation analysis of the 2017 dense water formation events: Climate change, bottom density currents, and Adriatic-Ionian Sea circulation (Mediterranean Sea). *Journal of Geophysical Research: Oceans*, *130*(11), 2024JC022306. https://doi.org/10.1029/2024JC022306

Masson-Delmotte, V., Zhai, P., Pirani, A., Connors, S. L., Péan, C., Berger, S.2023). *Climate change 2021: The physical science basis*. Cambridge University Press. https://doi.org/10.1017/9781009157896

Maze, G., & Balem, K. (2020). argopy: A python library for Argo ocean data analysis. *Journal of Open Source Software*, *5*(53), 2425. https://doi.org/10.21105/joss.02425

Pan, Y., Cheng, L., Abraham, J., Trenberth, K. E., Reagan, J., Du, J., et al. (2026). Ocean heat content sets another record in 2025. *Advances in Atmospheric Sciences*. https://doi.org/10.1007/s00376-026-5876-0

Parras-Berrocal, I. M., Vázquez, R., Cabos, W., Sein, D. V., Álvarez, O., Bruno, M., & Izquierdo, A. (2023). Dense water formation in the eastern Mediterranean under a global warming scenario. *Ocean Science*, *19*(3), 941–952. https://doi.org/10.5194/os-19-941-2023

Pinardi, N., Cessi, P., Borile, F., & Wolfe, C. L. P. (2019). The Mediterranean Sea overturning circulation. *Journal of Physical Oceanography*, *49*(7), 1699–1721. https://doi.org/10.1175/JPO-D-18-0254.1

Richon, C., Dutay, J.-C., Bopp, L., Le Vu, B., Orr, J. C., Somot, S., & Dulac, F. (2019). Biogeochemical response of the Mediterranean Sea to the transient SRES-A2 climate change scenario. *Biogeosciences*, *16*(1), 135–165. https://doi.org/10.5194/bg-16-135-2019

Rixen, M., Beckers, J., Levitus, S., Antonov, J., Boyer, T., Maillard, C., et al. (2005). The Western Mediterranean Deep Water: A proxy for climate change. *Geophysical Research Letters*, *32*(12). https://doi.org/10.1029/2005GL022702

Robinson, A., Malanotte-Rizzoli, P., Hecht, A., Michelato, A., Roether, W., Theocharis, A., et al. (1992). General circulation of the Eastern Mediterranean. *Earth-Science Reviews*, *32*(4), 285–309. https://doi.org/10.1016/0012-8252(92)90002-B

19448007, 2026, 18, Downloaded from https://agupubs.onlinelibrary.wiley.com/doi/10.1029/2026GL124518 by Cochrane Croatia, Wiley Online Library on [15/10/2026]. See the Terms and Conditions (https://onlinelibrary.wiley.com/terms-and-conditions) on Wiley Online Library for rules of use; OA articles are governed by the applicable Creative Commons License

Robinson, A. R., & Golnaraghi, M. (1994). The physical and dynamical oceanography of the Mediterranean Sea. In P. Malanotte-Rizzoli & A. R. Robinson (Eds.), *Ocean processes in climate dynamics: Global and mediterranean examples* (pp. 255–306). Springer. https://doi.org/10.1007/978-94-011-0870-612

Roemmich, D., Alford, M. H., Claustre, H., Johnson, K., King, B., Moum, J., et al. (2019). On the future of Argo: A global, full-depth, multi-disciplinary array. *Frontiers in Marine Science*, *6*, 439. https://doi.org/10.3389/fmars.2019.00439

Roether, W., Klein, B., Manca, B. B., Theocharis, A., & Kioroglou, S. (2007). Transient Eastern Mediterranean deep waters in response to the massive dense-water output of the Aegean Sea in the 1990s. *Progress in Oceanography*, *74*(4), 540–571. https://doi.org/10.1016/j.pocean.2007.03.001

K. Schroeder & J. Chiggiato (2023). *Oceanography of the Mediterranean Sea: An introductory guide*. Elsevier. https://doi.org/10.1016/C2020-0-00371-3

Schroeder, K., Chiggiato, J., Josey, S. A., Borghini, M., Aracri, S., & Sparnocchia, S. (2017). Rapid response to climate change in a marginal sea. *Scientific Reports*, *7*(1), 4065. https://doi.org/10.1038/s41598-017-04455-5

Skliris, N., Marsh, R., Breedon, M., & Josey, S. A. (2024). Accelerated warming and salinification of the Mediterranean Sea: Implications for dense water Formation. *Journal of Marine Science and Engineering*, *13*(1), 25. https://doi.org/10.3390/jmse13010025

Somot, S., Houpert, L., Sevault, F., Testor, P., Bosse, A., Taupier-Letage, I., et al. (2018). Characterizing, modelling and understanding the climate variability of the deep water formation in the North-Western Mediterranean Sea. *Climate Dynamics*, *51*(3), 1179–1210. https://doi.org/10.1007/s00382-016-3295-0

Somot, S., Sevault, F., & Déqué, M. (2006). Transient climate change scenario simulation of the Mediterranean Sea for the twenty-first century using a high-resolution ocean circulation model. *Climate Dynamics*, *27*(7–8), 851–879. https://doi.org/10.1007/s00382-006-0167-z

Soto-Navarro, J., Jordá, G., Amores, A., Cabos, W., Somot, S., Sevault, F., et al. (2020). Evolution of Mediterranean Sea water properties under climate change scenarios in the Med-CORDEX ensemble. *Climate Dynamics*, *54*(3–4), 2135–2165. https://doi.org/10.1007/s00382-019-05105-4

Storto, A., & Yang, C. (2024). Acceleration of the ocean warming from 1961 to 2022 unveiled by large-ensemble reanalyses. *Nature Communications*, *15*(1), 545. https://doi.org/10.1038/s41467-024-44749-7

Tan, Z., Von Schuckmann, K., Speich, S., Bopp, L., Zhu, J., & Cheng, L. (2026). Observed large-scale and deep-reaching compound ocean state changes over the past 60 years. *Nature Climate Change*, *16*(1), 58–68. https://doi.org/10.1038/s41558-025-02484-x

Terzić, E., Cardin, V., Le Meur, J., Dunić, N., Vodopivec, M., & Vilibić, I. (2025). Unprecedented warming and salinization observed in the deep Adriatic. *Limnology and Oceanography Letters*, *10*(6), lol2.70051. https://doi.org/10.1002/lol2.70051

Terzić, E., Gardiol, C., & Vilibić, I. (2025). Surface saline lakes in the Mediterranean Sea. *Ocean Science*, *21*(4), 1441–1459. https://doi.org/10.5194/os-21-1441-2025

Terzić, E., & Vilibić, I. (2026a). Cleaned Adriatic in situ hydrographic data (1952–2023) for a Mediterranean thermohaline acceleration analysis [Dataset]. *Zenodo*. https://doi.org/10.5281/zenodo.20345373

Terzić, E., & Vilibić, I. (2026b). MedClim analysis code for Mediterranean thermohaline acceleration analysis [Software]. *Zenodo*. https://doi.org/10.5281/zenodo.20410481

Testor, P., Bosse, A., Houpert, L., Margirier, F., Mortier, L., Legoff, H., et al. (2018). Multiscale observations of deep convection in the Northwestern Mediterranean Sea during winter 2012–2013 using multiple platforms. *Journal of Geophysical Research: Oceans*, *123*(3), 1745–1776. https://doi.org/10.1002/2016JC012671

Tuel, A., & Eltahir, E. A. B. (2020). Why is the Mediterranean a climate change hot spot? *Journal of Climate*, *33*(14), 5829–5843. https://doi.org/10.1175/JCLI-D-19-0910.1

Verri, G., Furnari, L., Gunduz, M., Senatore, A., Santos da Costa, V., De Lorenzis, A., et al. (2024). Climate projections of the Adriatic Sea: Role of river release. *Frontiers in Climate*, *6*, 1368413. https://doi.org/10.3389/fclim.2024.1368413

von Schuckmann, K., Moreira, L., Cancet, M., Gues, F., Autret, E., Baker, J., et al. (2024). The state of the global ocean. *State of the Planet*, *4-osr8*, 1–30. https://doi.org/10.5194/sp-4-osr8-1-2024

Waldman, R., Brüggemann, N., Bosse, A., Spall, M., Somot, S., & Sevault, F. (2018). Overturning the Mediterranean thermohaline circulation. *Geophysical Research Letters*, *45*(16), 8407–8415. https://doi.org/10.1029/2018GL078502

Wang, S., Jing, Z., Wu, L., Sun, S., Chen, Z., Ma, X., & Gan, B. (2024). A more quiescent deep ocean under global warming. *Nature Climate Change*, *14*(9), 961–967. https://doi.org/10.1038/s41558-024-02075-2

19448007, 2026, 18, Downloaded from https://agupubs.onlinelibrary.wiley.com/doi/10.1029/2026GL124518 by Cochrane Croatia, Wiley Online Library on [15/10/2026]. See the Terms and Conditions (https://onlinelibrary.wiley.com/terms-and-conditions) on Wiley Online Library for rules of use; OA articles are governed by the applicable Creative Commons License